JOURNAL OF CATALYSIS **161,** 123–131 (1996)
ARTICLE NO. 0169

Catalytic CO Oxidation over Pt–Rh/γ-Al_2O_3 Catalysts

Yeping Cai, Harvey G. Stenger, Jr.,[1] and Charles E. Lyman*

*Departments of Chemical Engineering and *Materials Science and Engineering, Lehigh University, Bethlehem, Pennsylvania 18015*

Received March 17, 1995; revised January 22, 1996; accepted February 9, 1996

Catalytic CO oxidation was investigated over Pt, Rh, and Pt–Rh bimetallic catalysts supported on γ-Al_2O_3. Both dry and wet calcination procedures were performed to control Cl content in the final products. The catalysts were characterized with hydrogen chemisorption and analytical electron microscopy (AEM). A steady-state plug-flow reactor was used for activity measurement. An automated on-line gas chromatograph was employed to analyze CO, CO_2, and O_2. Based upon our previous findings, we were able to prepare catalysts with only Pt-rich or only Rh-rich particles. The Cl concentration in these catalysts did not affect activity significantly. In net-oxidizing conditions, platinum was found to be more active than rhodium. The presence of synergism depends upon a certain metal particle composition-size distribution of Pt-rich alloy particles. The current investigation has also demonstrated that feed composition and operating temperature have a strong influence on the presence of the synergistic effect. The possible mechanisms of the observed synergism are discussed.

INTRODUCTION

The catalytic oxidation of CO continues to receive great attention because of increased environmental concerns. Even though the reaction has been studied extensively over platinum (1–6), rhodium (4–9), and Pt–Rh bimetallic catalysts (10–16), there is no general consensus in the literature about the synergistic effect in the Pt–Rh catalytic system. Although some authors have reported that CO oxidation activity over a Pt–Rh catalyst was substantially higher than the activity of individual Pt or Rh (10, 11), several research groups have published data which did not support the presence of synergism (12–15). Anderson and Rochester (16) performed FTIR studies of CO/O_2 reaction over Pt–Rh/Al_2O_3 catalysts and have indicated that short range Pt–Rh interactions, for catalysts prepared by a simultaneous impregnation method, may reduce the tendency for oxide formation leading to loss of oxidation activity.

Our previous studies (17, 18) showed that the composition of Pt–Rh alloy particles depends upon the preparation procedure and the bulk average amount of Pt and Rh, which is consistent with a proposed miscibility gap in the Pt–Rh equilibrium phase diagram. With the aid of analytical electron microscopy and a proposed phase diagram, Pt–Rh catalysts were prepared with only Pt-rich or only Rh-rich particles instead of a bimodal particle composition distribution usually found in coimpregnation preparation (17). Kinetic investigations using these catalysts for $NO + CO$ and $NO + H_2$, two important reactions in environmental applications, gave a clear indication that only the Pt-rich catalyst exhibited a synergistic effect for both reactions. In an effort to further understand the performance of Pt–Rh bimetallic catalysts, we present here our recent findings for the $CO + O_2$ reaction over various Pt–Rh catalysts.

In the present study, the carbon monoxide oxidation reaction was investigated over Pt–Rh/γ-Al_2O_3 catalysts. The activity of these bimetallic catalysts was compared to that of monometallic catalysts which contained only Pt or Rh. The objective of this investigation is to determine whether our previous findings, which related measured kinetic properties to the compositions of individual alloy particles, can be applied to the CO oxidation reaction. The effect of chlorine content, which may be an important parameter in determining catalyst activity and dispersion (12, 19, 20), is also reported.

EXPERIMENTAL

Catalyst Preparation

Aqueous solutions of Pt and Rh were prepared from $PtCl_4$ (99.9%, Johnson Matthey) and $RhCl_3 \cdot xH_2O$ (99.9%, Johnson Matthey), respectively. These precursors were impregnated into γ-Al_2O_3 (Corning Celcor EX78) which was ground and sieved to between 90 and 150 μm in diameter. The surface area of the support material was 252 m^2/g with a pore volume of 0.5 cc/g. The average pore size provided by the manufacturer was 4 nm. Before impregnation at room temperature, the precursor solution was filtered and then brought into contact with alumina. The resulting slurry was rinsed with water, dried in air overnight, and then calcined in air at 500°C for 4 h. The bimetallic catalysts were prepared by a sequential impregnation procedure (Pt impregnation followed by Rh impregnation) with drying (room

[1] To whom correspondence should be addressed.

0021-9517/96 $18.00

temperature, overnight) and calcination (500°C, 4 h) after each impregnation step. Two samples, labeled Pt (wet) and Rh (wet), were calcined at 500°C for 4 h in an air stream saturated with water (about 2%) by flowing the calcination air through a bubbler operated at room temperature. The metal contents were verified by inductively coupled plasma atomic emission spectroscopy (Galbraith Laboratories). Chlorine contents were also analyzed for some of the catalyst samples (Galbraith Laboratories). A catalyst which contained 0.78 wt% of Pt and 0.03 wt% of Rh would be designated as 96/4. Our intended bimetallic catalyst compositions were 98/2, 95/5, 90/10, and 50/50. The ICP analyses showed that the actual compositions were 99/1, 96/4, 93/7, and 69/31, respectively.

Catalyst Characterization

Analytical electron microscopy was performed using a Fisons Vacuum Generators HB-603 field-emission scanning transmission electron microscope (STEM) (21, 22). Platinum M-series (Mα, 2.051 keV) and rhodium L-series (Lα, 2.696 keV) X-rays were measured using an Oxford Instruments Si(Li) energy dispersive spectrometer with a Link Systems eXL X-ray analyzer. The STEM was operated at 300 kV and at conditions to provide approximately 0.5 nA of current into an electron probe 2 nm in diameter (full width at 1/10th maximum intensity). Since the 2 nm probe was rastered in a 3 × 4-nm rectangle, particles that were less than 3 nm in diameter were sampled over their entire volume, and particles larger than 3 nm in diameter were analyzed through their center. The analysis was performed using a rastered beam to allow direct observation of the particle during the process. X-rays were acquired for life times of 200 s per particle in order to achieve acceptable counting statistics. Net X-ray counts above background for a typical Pt-rich particle of 4 nm diameter were 8446 and 404 for Pt and Rh, respectively.

Metallic dispersion was determined by nonstatic chemisorption using a modified Micromeritics Flowsorb II 2300. A catalyst sample size of 0.5 g was reduced in flowing H_2 (minimum purity, 99.999%; MG Industries) at 150°C for 30 min, 250°C for 30 min, and 350°C for 2 h, followed by cooling to room temperature in a nitrogen environment. Chemisorption was performed by pulsing hydrogen in a nitrogen carrier with the assumption of metal to hydrogen ratio of 1 : 1. This assumed stoichiometry is generally accepted in literature (8, 12, 17). For replicate analyses of the same material, after chemisorption, the sample was heated to 350°C under flowing nitrogen and kept at 350°C for 30 min. The sample was cooled to room temperature and reanalyzed. Since H_2 adsorbs on both Pt and Rh, it was not possible to measure the number of Pt and Rh independently. Only the total number of surface sites could be determined. The accuracy of this technique was verified using a Pt chemisorption standard obtained from Micromeritics. On two separate days the standard sample with a specified dispersion of $33.7 \pm 5\%$ was measured to be 35.8 and 30.8%, respectively. We did not use CO chemisorption because of the uncertainties associated with the adsorption stoichiometry of CO on Rh (23–26).

Kinetic Studies

The apparatus used for the CO oxidation reaction was described previously (18). The feed gases consisted of 1.02% CO in He (MG Industries, certified), 1.95% O_2 in He (MG Industries, certified), pure O_2 (MG Industries, ultrahigh purity), and pure He (MG Industries, ultrahigh purity). The gas flow rates were controlled by three rotometers (Brooks, Sho-Rate). A back pressure regulator was used to maintain a constant pressure of 10 psig in the flow meter section of the system. A desired feed mixture was directed into a fused silica reactor, which measured 10 mm i.d. × 40 cm in length. The sample powder was supported on a fused silica frit located in the middle of the reactor. A type-K thermocouple was inserted axially down the reactor and placed in the catalyst bed. Gas analyses were achieved using a Carle 111 H dual column GC equipped with a $7' \times \frac{1}{8}''$ Haysep D column and a $15' \times \frac{1}{8}''$ Carboxen 1000 column. A Zenith Z-158 personal computer running Control EG software (Quinn-Curtis) was employed to control bed temperature and switch the GC on and off. The reaction temperature was controlled within 1/10th of a degree of a set point.

CO oxidation was performed at a temperature range of 60 to 300°C. Various stepwise temperature increments were programmed using Control EG. At each desired temperature, a couple of GC analyses were performed to ensure that steady state was reached. The temperature was then increased to the next set point. The CO concentration varied from 0.1 to 1.0%, whereas the O_2 concentration ranged from 0.5 to 5.0%. In most cases, the total flow rate was set at a constant value of 110 cm^3(STP)/min, although a high flow rate of 330 cm^3(STP)/min was also investigated. In the case of the high flow rate, a valve located at the exit of the reactor was equipped to allow only a portion of the gas stream into the GC sample loop. The purpose of venting part of the gas stream was to maintain a constant reactor pressure. Two sample sizes, 1.0 and 0.1 g, were selected in this study. A blank run with bare alumina was always performed prior to actual catalyst testing. The results obtained from kinetic experiments were reproducible within 5%.

RESULTS

Catalyst Characterization

Metal dispersions measured by H_2 chemisorption are summarized in Table 1. The pure Pt and the Pt-rich catalysts (99/1, 96/4, and 93/7) were found to have a dispersion of 100%. The pure Rh catalyst, calcined in a dry air stream, was

TABLE 1

Metal Dispersion Measured by Hydrogen Chemisorption and Chlorine Concentration under Dry and Wet Calcination Conditions

Catalyst	Bulk composition (wt%)	Calcination cond.	Cl content (wt%)	Dispersion (%)
Pt (fresh)	0.78 Pt	Prior to calcination	0.54	
Pt (dry)	0.78 Pt	Calcined, dry	0.51	100
Pt (wet)	0.78 Pt	Calcined, wet	0.34	100
Rh (fresh)	0.36 Rh	Prior to calcination	0.56	
Rh (dry)	0.36 Rh	Calcined, dry	0.52	45
Rh (wet)	0.36 Rh	Calcined, wet	0.31	38
99/1	0.78 Pt + 0.01 Rh	Calcined, dry		100
96/4	0.78 Pt + 0.03 Rh	Calcined, dry		100
93/7	0.78 Pt + 0.06 Rh	Calcined, dry		100
69/31	0.40 Pt + 0.18 Rh	Calcined, dry		70

found to have a dispersion value of 45%, slightly higher than the 38% obtained for the pure Rh catalyst calcined with a moist air stream. The 69/31 catalyst was found to have a 70% dispersion. The results were reproducible within experimental error. For the Rh (wet) catalyst, two almost identical values (38.0 and 38.1%) were obtained by the two consecutive analyses.

Analytical electron microscopy results for the 96/4 catalyst after catalytic testing are presented in Fig. 1. This plot of Pt composition (measured as X-ray intensity ratio) versus particle size shows that all particles analyzed were Pt-rich and between 3 and 7 nm in diameter. Particles having less than 3 nm in diameter are likely but not able to be detected. The small variation in composition with metal particle size has been shown to be related to segregation of Rh to the particle surface (27).

Kinetic Studies

Catalyst activity for the oxidation of CO to CO_2 is measured either by a light-off curve (CO conversion versus temperature) or by a value of T_{50} (temperature required to reach 50% conversion). The catalyst samples tested in the current studies are 100/0 (0.78% Pt), 99/1, 96/4, 93/7, 69/31, and 0/100 (0.36% Rh). The amount of catalyst was chosen to be equal for each set of reactions and, except for the Rh and 69/31 catalysts, the other catalysts have a dispersion of 100%. Thus, in most cases, the comparison of light-off curves or T_{50} values reflects the specific catalyst activity, that is, the catalyst turnover frequency (mole of CO reacted/site · s). The specific catalyst activity, however, is calculated for some of the selected data by using dispersion values found in Table 1. This is especially important in comparing catalyst samples with different metal dispersions.

The effect of Cl content on CO oxidation activity was investigated over the Pt and Rh monometallic catalysts. According to the procedure described by Castro *et al.* (28), we were able to regulate the final Cl levels in solids by controlling the calcination environment. Table 1 lists Cl concentrations under different calcination conditions. A normal calcination process involving dry air at 500°C for 4 h gave Cl contents of 0.51% for the Pt and 0.52% for the Rh, which were decreased from 0.54 and 0.56%, respectively, prior to

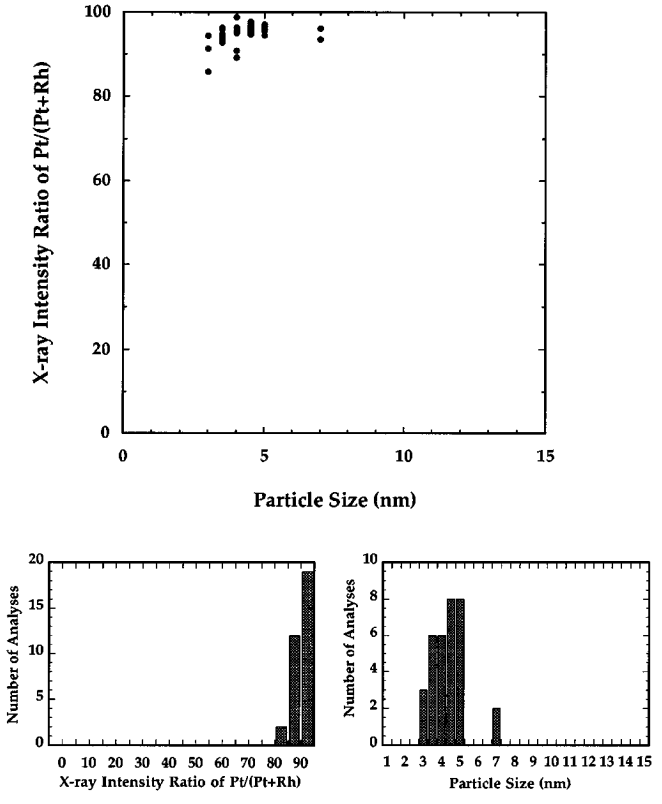

FIG. 1. Plot of particle composition (measured as X-ray intensity ratio) versus size for the 96/4 catalyst. Particle composition and particle size histograms are also presented.

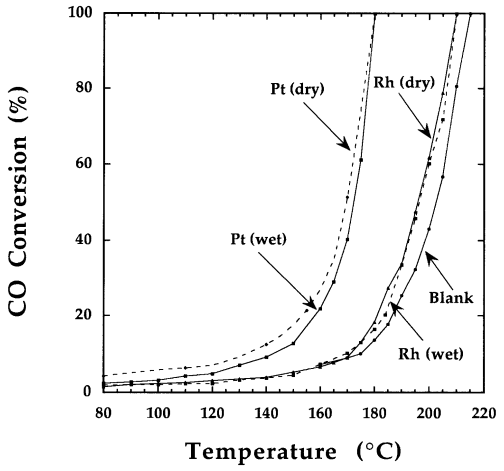

FIG. 2. CO conversion versus temperature over the Pt and Rh monometallic catalysts calcined in either a dry or a wet air stream. The experiments were performed at a CO concentration of 0.1% and an O_2 to CO ratio of 5 with a total flow rate of 110 cm^3/min. A sample size of 1.0 g was used.

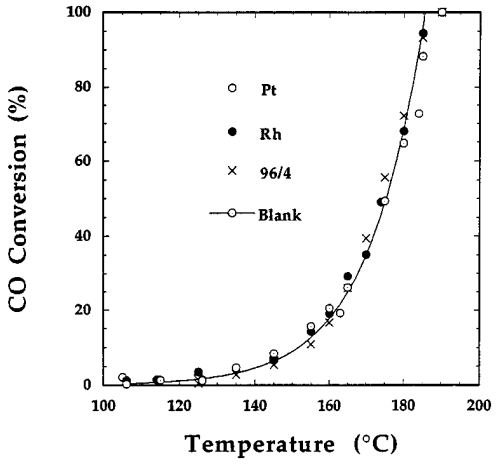

FIG. 3. CO conversion versus temperature at a CO concentration of 0.1% and an O_2 to CO ratio of 50 with a total flow rate of 110 cm^3/min. A sample size of 1.0 g was used.

the calcination. A significant loss of chlorine was observed if the samples went through a wet calcination process. Figure 2 shows CO oxidation activities of the samples with high [Pt (dry) and Rh (dry)] and low [Pt (wet) and Rh (wet)] chlorine levels. The experiment was performed at a CO concentration of 0.1% and an O_2/CO ratio of 5. All samples exhibit negligible activity at temperatures below 100°C. The Pt catalyst is significantly more active than the Rh sample, with its T_{50} value about 22°C lower than that of the Rh catalyst. The Arrhenius plot (not shown), which relates turnover frequency to inverse temperature, indicates an order of magnitude higher reaction rate constant for Pt than for Rh. The chlorine concentration does not appear to affect the catalyst activity significantly although a small difference in activity is observed between the Pt (dry) and the Pt (wet) catalysts. Both Pt catalysts show a complete conversion of CO at a temperature of 180°C, whereas temperatures higher than 210°C are required to reach a 100% conversion for the Rh samples. The actual temperature difference at a full ignition level (100% conversion) is greater if contributions from the blank run are considered. As is shown in Fig. 2, the homogeneous reaction of $CO + O_2$ affects the performance of Rh catalyst much more than that of Pt catalyst. If there were no homogeneous reaction involved, the temperature required to reach a 100% conversion (T_{100}) for the Rh catalyst would be much higher than 210°C, whereas the T_{100} of Pt would be slightly higher than 180°C.

The CO conversion versus temperature data obtained at a CO concentration of 0.1% are presented in Fig. 3 (O_2/CO = 50) and Fig. 4 (O_2/CO = 5). In the strong oxidizing condition (O_2/CO = 50), the blank run is identical to the reactions with catalysts. This is evidenced by a common light-off curve for the blank experiment and the actual catalyst testing. As shown in Fig. 3, experimental data obtained for the Pt, Rh, and 96/4 catalysts are scattered around a curve formed by the blank run. Thus, under these conditions the catalysts tested had negligible activity for converting CO to CO_2. The CO conversions obtained from the blank reactor run are attributed to the homogeneous reaction of CO with O_2. The bare alumina and the thermocouple were tested to have negligible activity within the temperature range studied. By reducing the ratio of O_2/CO to 5, more distinct differences in activity among the catalysts appears as illustrated in Fig. 4. The Pt catalyst displays the highest activity, followed by the 96/4, 99/1, and 93/7 catalysts. The Rh and 69/31 samples are the least active with their T_{50}

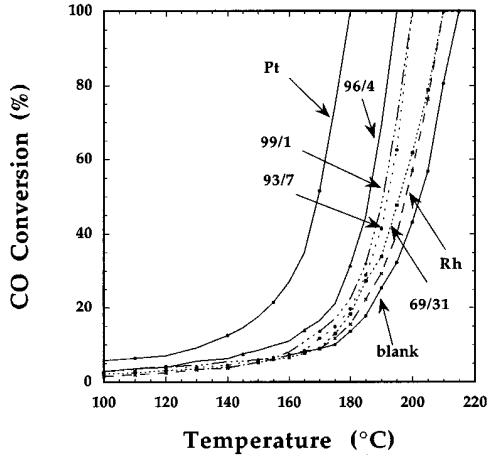

FIG. 4. Comparison of CO conversion curves of Pt, Rh, and various Pt–Rh bimetallic catalysts at a CO concentration of 0.1% and an O_2 to CO ratio of 5 with a total flow rate of 110 cm^3/min. A sample size of 1.09 g was used.

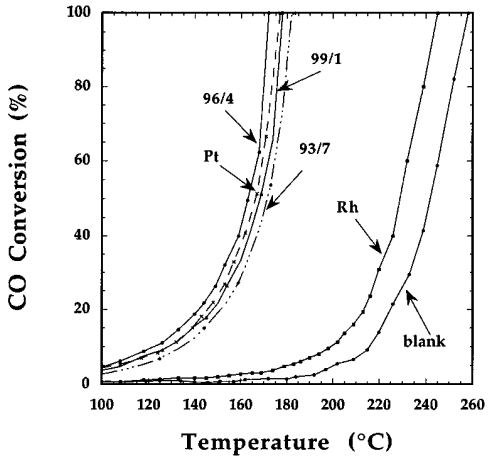

FIG. 5. Comparison of CO conversion curves of Pt, Rh, and various Pt–Rh bimetallic catalysts at a CO concentration of 0.5% and an O_2 to CO ratio of 2 with a total flow rate of 110 cm^3/min. A sample size of 1.0 g was used.

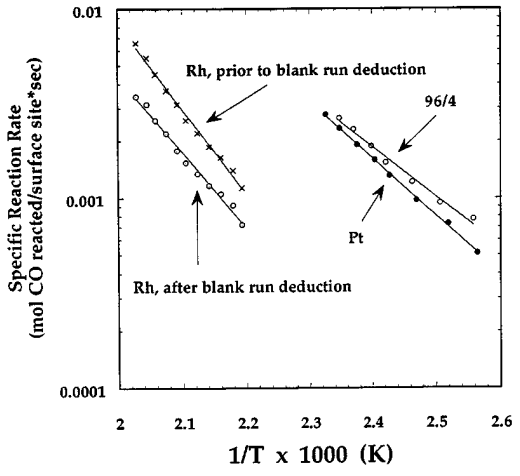

FIG. 6. Plot of specific reaction rates of Pt, Rh, and 96/4 catalysts versus inverse temperature at a CO concentration of 0.5% and an O_2 to CO ratio of 2 with a total flow rate of 110 cm^3/min. A sample size of 1.0 g was used.

values only 5°C lower than that of the blank run. The three bimetallic catalysts (96/4, 99/1, 93/7) perform better than Rh but not as well as Pt, and the fourth catalyst (69/31) has roughly the same activity as the Rh sample; thus, we can conclude that there are no synergistic effects observed under these experimental conditions.

Experiments with a CO concentration of 0.5% and an O_2/CO ratio of 2 provide increased activity for the bimetallic catalysts, which is illustrated in Fig. 5. The monometallic catalysts, however, either have a similar light-off curve (Pt) or display a lower activity (Rh) (Fig. 5 versus Fig. 4). Experiments under these reaction conditions were not performed over the 69/31 catalyst. According to our previous findings (17, 18), the 69/31 catalyst is expected to behave like Rh. The most interesting phenomenon from this investigation is that the 96/4 catalyst displays a greater activity than the Pt catalyst and thus exhibits synergism. The 99/1 and 93/7 catalysts, however, show activities within the boundary formed by the Pt and Rh monometallic catalysts. A similar run over the Pt and 96/4 catalysts with CO = 1% and O_2/CO = 2 gave the same difference in T_{50} values as shown in Fig. 8, confirming our observation in synergism.

An Arrhenius plot, which relates the specific activities of Pt, Rh, and 96/4 catalysts to inverse temperature under the conditions found in Fig. 5, is illustrated in Fig. 6. The specific rate is defined as the number of moles of CO converted per second per surface site. The number of surface site is calculated with the dispersion data found in Table 1. Experimental data with CO conversion levels less than 30% are considered in the figure. Two sets of data are plotted for Rh catalyst; one with the consideration of blank run contribution and the other without taking into account the blank experiment. There is no need to consider the blank run contribution to Pt and 96/4 catalysts since, at CO conversions less than 30% ($T < 155$°C), the homogeneous activity is negligible. A simple method, which involves subtracting blank run CO conversion at a specific temperature from CO conversion obtained with catalyst at the same temperature, is applied to the Rh catalyst. After the blank run deduction, the specific reaction rate is expected to be lower than that without blank run deduction. Regardless of blank run deduction, Rh is found to be an order of magnitude lower in activity than the Pt and 96/4 catalysts. The specific reaction rate is observed to be slightly higher for 96/4 than for Pt, being in consistent with comparisons using the light-off curve or the T_{50} value.

Further kinetic investigations were conducted to find conditions of more pronounced synergistic effects. Figure 7

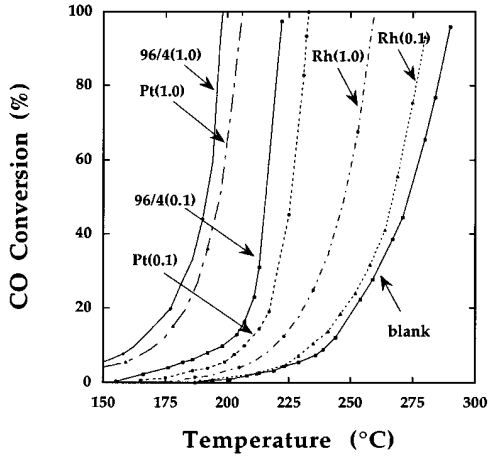

FIG. 7. Comparison of CO conversion curves of Pt, Rh, and 96/4 catalysts at a CO concentration of 0.5% and an O_2 to CO ratio of 2 with a total flow rate of 330 cm^3/min. The amount of catalyst used in the reaction is indicated in parentheses.

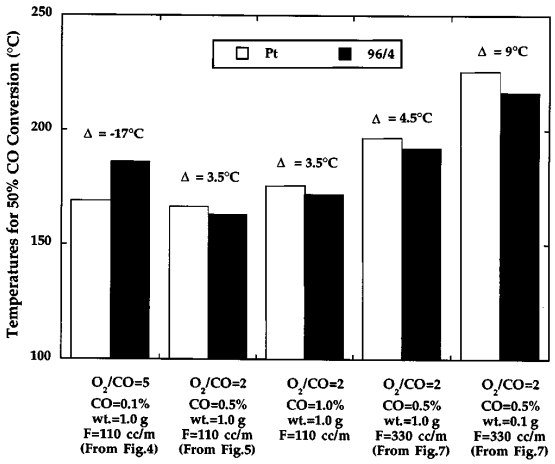

FIG. 8. Comparison of temperatures required to reach 50% CO conversion under various reaction conditions for Pt and 96/4 catalysts. The difference in T_{50} (T_{50} of Pt minus that of 96/4) is indicated as the Δ value.

presents the conversion data obtained at a total flow rate of 330 cm^3 (STP)/min with a CO concentration of 0.5% and an O_2/CO ratio of 2. The amount of the catalysts was either 1.0 or 0.1 g, and is indicated in parentheses. The theoretical criteria proposed in the literature (29) were applied to ensure that, under the current conditions, both internal and external mass transfer limitations did not exist. With the increase of space velocity, it was expected that CO conversion would shift to higher temperatures. In the case of the 1.0 g sample, an increase of approximately 25°C in T_{50} is observed for the three tested catalysts (96/4, Pt, Rh) as a result of tripling the total flow rate. When keeping the high flow rate and simultaneously reducing the sample size to 1/10th of the original, the temperature required to reach a 50% conversion is about 50°C higher than that shown in Fig. 5. An interesting phenomenon illustrated in Fig. 7 is that at increasing T_{50} values (hence decreasing catalyst activity), the observed difference in T_{50} levels of the Pt and 96/4 catalysts increases. Within our experimental range, the most pronounced synergism, in terms of T_{50} level, is observed to be 9°C lower for the 96/4 catalyst than for the Pt catalyst. Figure 8 summarizes the temperatures required to reach 50% CO conversion under various reaction conditions for the 96/4 and Pt catalysts.

DISCUSSION

The current study shows complete dispersion of the Pt and Pt-rich bimetallic catalysts (99/1, 96/4, 93/7). The highly dispersed Pt catalysts prepared by a calcination procedure are expected based on previous work (19). The 93/7 catalyst tested in this study contains a rhodium content of 0.06 wt%, which appears not to have affected the metal dispersion significantly. By comparing with our previous catalysts (17), which were prereduced in H_2 instead of preoxidized in air, it appears that the rhodium particle dispersion does not change significantly with pretreatment environment. A Rh metal dispersion of 41% was obtained when it was prereduced in H_2 (17), which is compared to 45 and 38% for calcination in dry air and wet air streams, respectively.

It is well established that sintered Pt or Rh metals can be redispersed by treatment with Cl-containing gases (12, 19, 30). Chlorine was reported to be retained by the catalyst even after reduction (31). This study has successfully demonstrated that the chlorine levels in catalysts can be controlled in the calcination process, and that a high chlorine concentration, which was obtained under a dry calcination condition, results in a slightly higher Rh dispersion. It is difficult to make a similar comparison for the Pt samples since they have a dispersion of 100%. High dispersions, however, do not necessarily correspond to a high catalytic activity. In fact, previous work showed that increased dispersion did not enhance CO oxidation activity over Rh and Pt–Rh catalysts (12, 16). Our study reveals no pronounced difference in activity between the samples with different Cl concentrations.

Our previous studies (17, 18) for the $NO + H_2$ and $NO + CO$ reactions demonstrated that a 95/5 catalyst, which contained only Pt-rich particles and had a Pt concentration in the range of 80 to 100 wt%, displayed activity higher than expected from the summation of Pt and Rh. We also showed that other bimetallic catalysts, although prepared by a similar method, did not show synergistic performance for either of the reactions due to a bimodal particle composition distribution. In the later catalysts both Pt-rich and Rh-rich particles were observed. The Rh-rich particles showed poor activity which negated the increased activity of the Pt-rich particles. The catalysts employed in our current investigations were prepared at temperatures and compositions to have a Pt-rich composition distribution over all particle sizes. This has been confirmed by our current AEM results for the 96/4 catalyst (Fig. 1).

The present CO oxidation kinetic studies demonstrate that the presence of synergism not only depends upon the particle composition distribution, but is also sensitive to the feed composition and the operating temperature. Our initial experiment with a ratio of O_2 to CO of 5 (Fig. 4) gives CO light-off curves for the bimetallic catalysts between those of the Pt and Rh monometallic catalysts, indicating the absence of synergistic effect. The positions of the conversion curves for the Pt/Rh catalysts are closer to Rh, with the 96/4 catalyst showing slightly higher activity than the other bimetallic catalysts. The order of catalytic activity is dramatically changed at an O_2 to CO ratio of 2 (Fig. 5). Under these conditions, the 96/4 catalyst has the highest activity, followed by the Pt, 99/1, and 93/7 catalysts. Rhodium, on the other hand, is the least active catalyst, with a T_{50} value 12°C lower than the blank run. The lower activity for Rh than for Pt and 96/4 is also illustrated in the

Arrhenius plot (Fig. 6). It is worth noting that this synergistic phenomenon is reproducible under similar reaction conditions: an O_2 to CO ratio of 2 and a CO concentration of 1% (Fig. 8).

One might argue that the slightly lower T_{50} values (3.5°C) of the 96/4 catalyst than the Pt sample could be attributed to experimental errors. This led us to find a more pronounced synergistic effect by varying the operating conditions (Fig. 7). Tripling the total flow rate and decreasing the sample size are both expected to move the temperature–conversion curve to higher temperatures. However, under theses conditions, the difference in activity between the Pt and the 96/4 catalysts increases, with the temperature required to reach a 50% conversion about 9°C lower for the 96/4 catalyst than for the Pt sample (0.1 g of sample). This is a significant improvement over the value of 3.5°C shown in Fig. 5 at lower operating temperatures. Due to experimental limitations, we are unable to operate the system at higher temperatures and at the same time avoid the homogeneous activity contributions.

Oh and Carpenter (10) presented convincing evidence in favor of CO oxidation synergism. Their preparation procedures, which led to the presence of synergism in the CO oxidation reaction, probably produced Pt-rich catalyst particles (18). In addition, Oh and Carpenter may have benefited from high operating temperatures caused by very low metal loading, high space velocity, and appropriate O_2 to CO ratio. The later is supported by their data obtained at a CO concentration of 1% and an O_2 to CO ratio of 5 (10). Under these conditions, they showed that the temperature required to reach 50% conversion was only 2°C lower for the Pt–Rh catalyst than for the monometallic Pt catalyst.

Some published data do not show activity enhancement by combining Pt and Rh (13–15, 32) Nieuwenhuys research group (13, 14) coimpregnated silica to produce Pt–Rh bimetallic catalysts with metal compositions of 25 at.% Rh, 50 at.% Rh, and 75 at.% Rh, which are likely to produce bimodal distributions of particle compositions (17). This particle microstructure can have many metal sites with low activity which would preclude synergism (18). In addition, although a high space velocity was used in their experiments, the catalysts with a high metal loading (7 wt%) oxidized CO at relatively low temperatures (13, 14). Thus, a relatively low operating temperature regime may also contribute to the absence of synergism. A recent paper by Anderson (15) provided experimental evidence which did not favor synergism for the CO oxidation reaction. Here the lack of activity enhancement for the Pt–Rh catalysts was explained by the absence of NO in the gas stream and/or the necessity of acetone solutions instead of aqueous environments in catalyst preparation. Anderson and Williams (32) reported that the light-off curve of the 0.5 wt% Pt–0.5 wt% Rh/γ-Al_2O_3 catalyst laid between those of the monometallic components and that acetone solutions in catalysts prepared by two-stage impregnation were likely to explain differences between single- and two-stage prepared Pt–Rh catalysts. Although evidence obtained in the present work is not broad enough to evaluate these nonsynergistic results, it is our belief that both the alloy particle composition–size distribution and the reaction conditions play a major role in the appearance of a synergistic effect for CO oxidation.

The synergistic effects shown in our data might be explained by the possibility that Rh reduction is promoted by the presence of Pt. It is well established that the reduced forms of Pt and Rh are more active in CO oxidation than their oxidized counterparts (9, 33). For oxidized Pt catalysts, it has been suggested that the CO oxidation reaction proceeds on reduced metal atoms and that only a small fraction of the metal is in the reduced and active state (33, 34). In an oxidizing environment (O_2/CO = 5) as shown in Fig. 4, both metals are expected to be oxides on the γ-Al_2O_3, and the overall reaction rate should be a summation of the rate over the Pt and the rate over the Rh. An averaged performance of the bimetallic Pt–Rh catalysts is expected. Decreasing the O_2/CO ratio to 2 perhaps partially reduces the Pt and bimetallic catalysts, but not the Rh-only catalyst. This observation is supported by a slightly dark color of the Pt and Pt-rich catalysts after the reaction. However, this does not happen for the Rh-only catalyst, suggesting that the oxidation state of the Rh did not change. For the bimetallic catalysts, however, Rh might be expected to be more easily reduced. This Rh reduction in the bimetallic catalysts is presumably influenced by the presence of Pt. Reduced Rh was shown to be more active for CO oxidation than reduced Pt (15). Thus the Pt–Rh alloy catalyst surface may be considered to consist of two separated active sites; a small amount of partially reduced Rh with high activity per site and a large amount of partially reduced Pt with relatively low activity. Consequently, the enhanced activity of the 96/4 catalyst relative to the pure Pt catalyst is not surprising. The lack of synergism for the 99/1 catalyst may simply be due to a relatively small enhancement in activity, which could not be observed in our experiment. Higher Rh concentration in a catalyst, such as in the 93/7, may create a scenario that the number of Pt atoms is not enough to meet the demands of a relatively large number of Rh atoms on the particle surface. As a result, the inactive rhodium oxide exposed on the surface decreases the overall activity. In an extreme case, such as in the 69/31 catalyst, Rh may completely cover the Pt atoms in the form of inactive rhodium oxide.

Another approach to explaining the observed synergism might be the selective adsorption effect, which reduces site competition and increases reaction rate by increasing the probability of having both reactant species on neighboring sites. Oh and Carpenter (10) proposed that the bimetallic catalyst surface is composed of randomly distributed Pt sites and Rh sites. The Pt atom acts as a CO adsorption site

while the Rh site selectively adsorbs oxygen. This results in reactive species bonding in close proximity and can lead to the enhancement of reaction rate for the bimetallic catalysts. This proposal was recently supported by Herz *et al.* (35) (using Monte Carlo techniques), who suggested that a composite material composed of two different sites, each with optimal properties for the adsorption of one reactant, would perform better than a single material. The bimetallic catalysts prepared in our laboratory can be visualized as an alloy containing both Rh sites and Pt sites. Our AEM results have revealed the formation of Pt–Rh alloy particles in the 96/4 catalyst. Under the current calcination conditions, the Pt–Rh alloy is expected to have surface partially enriched with Rh (36–38). For a similar catalyst investigated previously (18), the maximum Rh surface composition was estimated to be 30 at.% if a complete Rh segregation was assumed. Pt surface was reported to hold CO more strongly (1). Based on the findings by Zhu and Schmidt (38), oxygen treatment completely suppressed CO chemisorption on Rh. Oxygen was known to adsorb much more strongly on a clean Rh surface than CO (39, 40). Thus the surface of our bimetallic catalysts can be thought to contain a statistical mixture of sites with the property of selective adsorption. The resulting adsorbed CO on a Pt site would react with the neighboring Rh adsorbed oxygen species, and an enhancement in activity for the bimetallic catalysts would be expected.

As we reported earlier (17, 18), a Pt-rich particle composition distribution is necessary to observe the synergistic effect. In the current investigation, we have demonstrated that synergism, in CO oxidation, is also sensitive to reaction conditions, specifically to the feed composition and the operating temperature. Reaction temperature is influenced by parameters such as metal loading, total flow rate, volume of the heating zone, and catalyst oxidation state. The oxidation states of a catalyst can significantly affect the operating temperature. In a separate experiment, prereduced Pt and Rh catalysts were tested for their CO oxidation activity. These catalysts were reduced in flowing pure H_2 at 350°C for 12 h, and were subjected to the same reaction conditions as those in Fig. 4 (0.5 g instead of 1.0 g). Complete CO conversion at about 100°C was obtained initially for both reduced Pt and reduced Rh (Rh was more active), which is significantly lower than the 180 to 210°C needed for the oxidized catalysts. However, the activity of these catalysts was not stable, and, after several hours the activity approached the level of the preoxidized samples. It is important, therefore, to perform CO oxidation experiments in a stable oxidation state for a catalyst in order to fully understand the mechanism of synergistic effect. Jernigan and Somorjai (41) studied CO oxidation reaction over copper catalysts rather than Pt–Rh. They have reported that the surface oxidation state changes as a function of gas composition, reaction temperature, as well as exposure time, and have successfully showed that stable copper oxidation state can be obtained and maintained by varying the O_2/CO ratio. Experiments that control the oxidation states of Pt, Rh, and Pt–Rh bimetallic catalysts are currently underway to investigate kinetic performance of different oxidation states of Pt and Rh, as well as the possible mechanism of Rh reduction in the presence of Pt.

CONCLUSIONS

Platinum–rhodium alloy catalyst particles, with a uniform Pt-rich composition distribution, exhibit synergistic effects for CO oxidation. However, the presence of synergism not only depends on the particle composition distribution, but it is also sensitive to the feed composition and the operating temperature. Two possible mechanisms for the observed synergism have been discussed: the partially reduced Rh effect and the selective adsorption effect.

ACKNOWLEDGMENTS

This work is supported by U.S. Department of Energy under Contract DE-FG02-86ER45269. The authors also thank D. W. Ackland for assistance in analytical electron microscopy and Tony Rutch for assistance in catalytic testing.

REFERENCES

1. McCarthy, E., Zahradnik, J., Kuczynski, G. C., and Carberry, J. J., *J. Catal.* **39**, 29 (1975).
2. Cant, N. W., *J. Catal.* **62**, 173 (1980).
3. Sarkany, J., Bartok, M., and Gonzalez, R., *J. Catal.* **81**, 347 (1983).
4. Cant, N. W., Hicks, P. C., and Lennon, B. S., *J. Catal.* **54**, 372 (1978).
5. Yu Yao, Y.-F., *J. Catal.* **87**, 152 (1984).
6. Engel, T., and Ertl, G., *in* "Advances in Catalysis" (D. D. Eley, H. Pines, and P. B. Weisz, Eds.), Vol. 28, p.1. Academic Press, New York, 1979.
7. Goodman, D. W., and Peden, C. H. F., *J. Phys. Chem.* **90**, 4839 (1986).
8. Oh, E. H., and Eickel, C. C., *J. Catal.* **128**, 526 (1991).
9. Kiss, J. T., and Gonzalez, R. D., *J. Phys. Chem.* **88**, 898 (1984).
10. Oh, S. H., and Carpenter, J. E., *J. Catal.* **98**, 178 (1986).
11. Tzou, M. S., Asakura, K., Yamazaki, Y., and Kuroda, H., *Catal. Lett.* **11**, 33 (1991).
12. D'Aniello, M. J., Jr., Monroe, D. R., Carr, C. J., and Krueger, M. H., *J. Catal.* **109**, 407 (1988).
13. Van Den Bosch-Driebergen, A. G., Kieboom, M. N. H., Van Dreumel, A., Wolf, R. M., Van Delft, F. C. M. J. M., and Nieuwenhuys, B. E., *Catal. Lett.* **2**, 73 (1989).
14. Wolf, R. M., Siera, J., Van Delft, F. C. M. J. M., and Nieuwenhuys, B. E., *Faraday Discuss. Chem. Soc.* **87**, 275 (1989).
15. Anderson, J. A., *J. Catal.* **142**, 153 (1993).
16. Anderson, J. A., and Rochester, C. H., *Catal. Today* **10**, 275 (1991).
17. Lakis, R. E., Lyman, C. E., and Stenger, H. G., Jr., *J. Catal.* **154**, 261 (1995).
18. Lakis, R. E., Cai, Y., Lyman, C. E., and Stenger, H. G., Jr., *J. Catal.* **154**, 276 (1995).
19. Straguzzi, G. I., Aduriz, H. R., and Gigola, C. E., *J. Catal.* **66**, 171 (1980).
20. Bazin, D., Dexpert, H., Lagarde, P., and Bournonville, J. P., *J. Catal.* **110**, 209 (1988).

21. Lyman, C. E., Goldstein, J. I., Williams, D. B., Ackland, D. W., Von Harrach, S., Nicholls, A. W., and Statham, P., *J. Microsc.* **176**, 85 (1994).
22. Lyman, C. E., Lakis, R. E., and Stenger, H. G., *Ultramicroscopy* **58**, 25 (1995).
23. Cavanagh, R. R., and Yates, J. T., Jr., *J. Chem. Phys.* **74**, 4150 (1981).
24. Yates, D. J. C., Murrell, L. L., and Prestridge, E. B., *J. Catal.* **57**, 41 (1979).
25. Worley, S. D., Rice, C. A., Mattson, G. A., Curtis, C. W., Guin, J. A., and Tarrer, A. R., *J. Chem. Phys.* **76**, 20 (1982).
26. Yao, H. C., and Rothschild, W. G., *J. Chem. Phys.* **68**, 4774 (1978).
27. Lakis, R. E., Lyman, C. E., and Stenger, H. G., *in* "Proceedings of the Microscopy Society of America" (G. W. Bailey and A. J. Garratt-Reed, Eds.), p. 780. San Francisco Press, San Francisco, 1994.
28. Castro, A. A., Scelza, O. A., Benvenuto, E. R., Baronetti, G. T., and Parera, J. M., *J. Catal.* **69**, 222 (1981).
29. Carberry, J. J., "Chemical and Catalytic Reaction Engineering." McGraw–Hill, New York, 1976.
30. Foger, K., and Jaeger, H., *J. Catal.* **92**, 64 (1985).
31. Johnston, P., and Joyner, R. W., "Catalysis and Surface Characterization" (T. J. Dines, C. H. Rochester, and J. Thomson, Eds.), p. 51. Royal Society of Chemistry, London, 1992.
32. Anderson, J. A., and Williams, B., "Catalysis and Surface Characterization" (T. J. Dines, C. H. Rochester, and J. Thomson, Eds.), p. 136. Royal Society of Chemistry, London, 1992.
33. Herz, R. K., and Marin, S. P., *J. Catal.* **65**, 281 (1980).
34. Herz, R. K., and Shinouskis, E. J., *Appl. Surf. Sci.* **19**, 373 (1984).
35. Herz, R. K., Badlani, A., Schryer, D. R., and Upchurch, B. T., *J. Catal.* **141**, 219 (1993).
36. Schmidt, L. D., and Wang, T., *J. Vac. Sci. Technol.* **18**(2), 520 (1981).
37. Poulston, S., and Smith, G. D. W., "Catalysis and Surface Characterization" (T. J. Dines, C. H. Rochester, and J. Thomson, Eds.), p. 228. Royal Society of Chemistry, London, 1992.
38. Zhu, Y., and Schmidt, L. D., *Surf. Sci.* **129**, 107 (1983).
39. Thiel, P. A., Williams, E. D., Yates, J. T., Jr., and Weinberg, W. H., *Surf. Sci.* **84**, 54 (1979).
40. Root, T. W., Schmidt, L. D., and Fisher, G. B., *Surf. Sci.* **134**, 30 (1983).
41. Jernigan, G. G., and Somorjai, G. A., *J. Catal.* **147**, 567 (1994).